Ab initio Study of Hydrazoic Acid

I. The Ground State: $HN_3(^1A')$

Jacques Lievin, Jacques Breulet*, and Georges Verhaegen

Laboratoire de Chimie Physique Moléculaire, CP. 160, Université Libre de Bruxelles, 50, ave. F. D. Roosevelt, B-1050 Brussels, Belgium

SCF and CI calculations were carried out on the ground $^1A'$ state of HN_3. The equilibrium geometry and vibration frequencies were computed. The results point to a planar structure (group C_s) but to a non-linear (170°) N—N—N conformation. The calculated vibration frequencies are in fair agreement with experimental assignments.

The dissociation path of the molecule to NH and N_2 products was investigated and compared to the isoelectronic reaction of diazomethane. The dissociation energy of hydrazoic acid is estimated to be about -8 kcal/mole, with a potential barrier to dissociation of about 30 kcal/mole.

Key words: Hydrazoic acid, electronic structure of ~

1. Introduction

Hydrazoic acid is quite an important reagent in organic chemistry, its main interest being its reaction with carboxylic acids to yield acyl azides, which in turn via a Schmidt degradation reaction lead to isocyanates [1]. Also, one of the important properties of this molecule is its low stability: it is known to explode very easily even under mild conditions [2].

The molecular properties of hydrazoic acid are not well known. The geometrical structure of the molecule has been determined partially only by microwave spectroscopy: the N—N and N—H distances as well as the N—N—H angle have been derived assuming that the molecule is planar and that the three N atoms are colinear [3]. Vibration frequencies have been determined by IR spectroscopy [4, 5]. The dissociation process $HN_3 \rightarrow NH + N_2$ has been discussed [6] on the basis of electron impact measurements.

---

* Boursier IRSIA

Calculations have been made to check the linearity of the N atoms: the results point to a quasi-linear structure, the N—N—N angle being 172° [7]. Other relevant calculations concern the K-shell binding energies [8, 9], other spectral properties of HN_3 [9], and the protonation of N_3^- [10]. All these calculations [7, 8, 10] were made with basis sets of variable size, except those of Rabalais *et al.* [9] which are semi-empirical (INDO).

In this work we shall report the results of *ab initio* calculations (SCF CI) for the ground state of the molecule along its dissociation path. The equilibrium geometry, vibration frequencies, dissociation path and intersystem crossing with an excited triplet state will be described. Of special interest will be the comparison of some of these quantities with those of the isoelectronic species diazomethane (CH_2N_2) which have been reported previously [11, 12], and those of the azide ion (N_3^-) to be reported here.

2. Methods of Calculation

2.1. Geometry

In Fig. 1, we give the axis convention adopted as well as the geometrical parameters which were varied in order to determine the equilibrium geometry and the dissociation path of HN_3. Since hydrazoic acid is experimentally reputed to be a non-linear but planar molecule [3], most calculations were made on point-group C_s structures; a few calculations only were performed in point-group C_1 symmetry ($\tau \neq 0$).

2.2. Electronic Configurations and States

From previous work [7–10] the ground configuration and state of HN_3 (group C_s) is known to be:

$$(1\text{–}6)a'^2\, 1a''^2\, (7\text{–}9)a'^2\, 2a''^2, \qquad {}^1A'$$

The dissociation products have configurations and states:

$$\text{NH(group } C_{\infty v}) \quad 1\sigma^2 2\sigma^2 3\sigma^2 1\pi^2, \qquad {}^3\Sigma^-, {}^1\Delta, {}^1\Sigma^+$$

$$\text{N}_2\text{(group } D_{\infty h}) \quad 1\sigma_g^2 1\sigma_u^2 2\sigma_g^2 2\sigma_u^2 1\pi_u^4 3\sigma_g^2, \qquad {}^1\Sigma_g^+$$
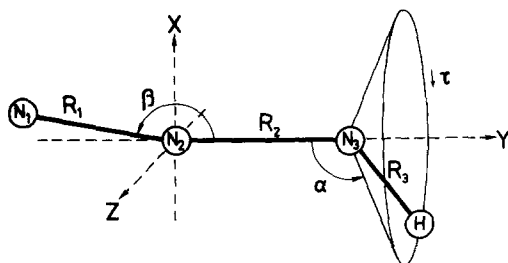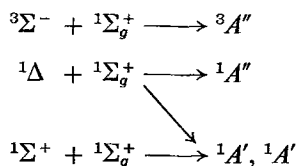

Fig. 1. Parameters and axis convention for HN_3; $\tau = 180°$ corresponds to a planar *trans* structure (point group C_s)

Combination of these configurations in group C_s yields:

$A:$ $(1-6)a'^2 1a''^2 (7-9)a'^2 2a''^2,$ $\qquad$ $^1A'$

$B:$ $(1-6)a'^2 1a''^2 (7-9)a'^2 2a'' 10a',$ $\qquad$ $^3A'', {}^1A''$

$C:$ $(1-6)a'^2 1a''^2 (7-9)a'^2 10a'^2,$ $\qquad$ $^1A'$

The electronic states for their part combine as:

$$^3\Sigma^- + {}^1\Sigma_g^+ \longrightarrow {}^3A''$$

$$^1\Delta + {}^1\Sigma_g^+ \longrightarrow {}^1A''$$

$$^1\Sigma^+ + {}^1\Sigma_g^+ \longrightarrow {}^1A', {}^1A'$$

Owing to the degeneracy of π_x and π_y orbitals in point group $C_{\infty v}$ symmetry, the two $^1A'$ states should be degenerate at the dissociation limit with an energy equal to that of $NH(\frac{1}{2}E(^1\Sigma^+) + \frac{1}{2}E(^1\Delta)) + N_2(E(^1\Sigma_g^+))$. Thus one expects that the ground configuration A will mix increasingly with configuration C as R_2 increases, until a 50% contribution of configuration C is achieved at the dissociation limit.

Also, since $^3\Sigma^-$ is the ground state of NH, one expects an intersystem crossing between the ground $^1A'$ state (Configurations A and C) and the $^3A''$ state (Configuration B).

2.3. Programs, Basis Sets, and Calculations

The SCF energies were obtained with the well-known program GAUSSIAN 70 [13]. The SCF equations were set up using the method of Roothaan [14] for closed-shell structures, and the method of Davidson (OCBSE) [15] for open-shell structures. The first of these methods is a part of GAUSSIAN 70, the second was coded by Morokuma and Iwata [16].

Preliminary calculations were made with the minimal STO-3G [17] basis set, production runs made use of the 6-31G [18] basis set of double zeta quality. Both of these sets are in-built to GAUSSIAN 70. A few calculations were also made with basis set 6-31G** [19] using GAUSSIAN 76 [20].

Configuration interaction (CI) calculations were run at different levels of approximation: the programs used are those written by Whitten and his collaborators [21] and extended (modified) by one of us (J. L.). These programs select amongst all possible configurations engendered by single or double substitution from the ground configuration those whose interaction with one (ground) or more chosen configurations is greater than a chosen threshold; the interaction is calculated from second order perturbation theory.

2.4. Equilibrium Geometry and Vibration Frequencies

The equilibrium geometry was obtained by fitting the energy values to coupled quadratic equations involving all the parameters. Coupling terms include all

possibilities between adjacent in-plane parameters (i.e. $R_1\beta$, R_1R_2, $R_2\beta$, $\alpha\beta$, $R_2\alpha$, $R_3\alpha$ and R_2R_3). A term in β^3 was also considered.

Vibration frequencies were obtained from direct diagonalization of the corresponding FG matrix. According to group-theoretical considerations, HN_3 has 5 normal modes of A' symmetry and one of A'' symmetry, the latter corresponding exclusively to the out-of-plane angle τ and reversely τ participating only to the A'' symmetry coordinate. Thus, if one uses internal coordinates (R_1, R_2, R_3, α, β and τ),

Table 1. Survey of some calculated points

Molecule (geometry)[a]	State	Basis set	CI calculation[b] δ	n	Energy (a.u.)
$HN_3(R_1 = 1.125\,\text{Å},$	$^1A'$	6-31G	—	—	−163.7292
$R_2 = 1.27\,\text{Å}, R_3 = 1.02\,\text{Å},$		6-31G	2.10^{-4}	594	−163.9145
$\alpha = 111°, \beta = 170°)$		6-31G	7.10^{-5}	1339	−163.9247
		6-31G**	—	—	−163.8392
$HN_3(\beta = 161°)$[c]	$^1A'$	6-31G	—	—	−163.7276
		6-31G	2.10^{-4}	567	−163.9110
		6-31G**	—	—	−163.8360
$HN_3(\beta = 181°)$[c]	$^1A'$	6-31G	—	—	−163.7271
		6-31G	2.10^{-4}	581	−163.9093
		6-31G**	—	—	−163.8376
$HN_3(\beta = 191°)$[c]	$^1A'$	6-31G	—	—	−163.7217
$HN_3(R_1 = 1.103\,\text{Å},$	$^1A'$	6-31G	—	—	−163.7098
$R_2 = 1.587\,\text{Å}, R_3 = 1.03\,\text{Å},$		6-31G	2.10^{-4}	563	−163.8829
$\alpha = 98°, \beta = 163°)$		6-31G	7.10^{-5}	1243	−163.8940
		6-31G**	—	—	−163.8054
	$^3A''$	6-31G	—	—	−163.6550
$HN_3(R_1 = 1.099\,\text{Å},$	$^1A'$	6-31G	—	—	−163.7084
$R_2 = 2.117\,\text{Å}, R_3 = 1.035\,\text{Å},$		6-31G	2.10^{-4}	333	−163.8686
$\alpha = 90°, \beta = 156°)$		6-31G	7.10^{-5}	693	−163.8851
		6-31G**	—	—	−163.7983
	$^3A''$	6-31G	—	—	−163.7768
$HN_3(R_1 = 1.094\,\text{Å},$	$^1A'$	6-31G	—	—	−163.7050
$R_2 = 3.2\,\text{Å}, R_3 = 1.035\,\text{Å},$		6-31G	7.10^{-5}	418	−163.8846
$\alpha = 90°, \beta = 156°)$	$^3A''$	6-31G	—	—	−163.8061
$NH(R = 1.032\,\text{Å})$	$\frac{1}{2}(^1\Delta + {}^1\Sigma^+)$	6-31G	—	—	−54.8357
		6-31G	7.10^{-5}	60	−54.8934
		6-31G**	—	—	−54.8538
	$^1\Delta$	6-31G	7.10^{-5} [d]	106	−54.9031
	$^3\Sigma^-$	6-31G	—	—	−54.9384
$N_2(R = 1.095\,\text{Å})$	$^1\Sigma_g^+$	6-31G	—	—	−108.8679
		6-31G**	—	—	−108.9430

[a] $\tau = 180°$ for all geometries considered here.

[b] δ refers to the threshold for selecting configurations, n is the corresponding number of configurations. Unless otherwise indicated, calculations are carried out on the $^1A'$ state (Configuration A) as reference state. SCF calculations are characterized by blanks.

[c] Same geometry as first point except for the value of angle β.

[d] CI reference state: $(1/\sqrt{2})(|\cdots\pi_x\bar{\pi}_x| - |\cdots\pi_y\bar{\pi}_y|)$, see Section 3.5.

the *FG* matrix is in this case block-diagonalized in two sub-matrices, one of dimension 5, the other of dimension 1 just as if symmetry coordinates had been used. All the *G* (kinetic energy) matrix elements are tabulated [22], the *F* (potential energy) matrix elements were deduced from the above-mentioned quadratic expansion.

2.5. Calculations

As there are far too many calculated points to list individually,[1] in Table 1 we merely give a list of the most important calculated points obtained with the extended basis sets 6-31G and 6-31G**, together with parallel CI results. These points correspond to the dissociation path on the one hand, and to a variation of angle β around its equilibrium value on the other hand.

3. Results and Discussion

3.1 Equilibrium Geometry

In Table 2 we compare the equilibrium values of the parameters found here with basis-sets STO-3G and 6-31G with the corresponding experimental values [3]. For the distances, the agreement is at worse ~ 0.03 Å with basis set 6-31G. It is interesting to note that, as in CH_2N_2 [11, 24], the distance between the non-neighbouring heavy atoms (last column of Table 2) is in better agreement with the experimental findings, than the individual bond-lengths. Likewise with basis set STO-3G, the value R_1 (N—N bound) is overestimated – this is entirely in keeping with similar findings in CH_2N_2.

The comparison between calculated and experimental values of the angles is made more difficult because the lack of experimental data made it necessary to *postulate* [3] a planar structure with three co-linear N atoms. Our findings confirm the postulated planar structure of the molecule, but not the linearity of the N atoms. In Table 3 we present values of β (cf. Fig. 1) calculated here at different levels of approximation together with the value proposed by Harrison *et al.* [7] from large basis set calculations, although this latter result does not proceed from a complete geometry optimization. All these theoretical data point to a non-linearity of 7–10°. This value is corroborated by similar results found for the isoelectronic molecule NHCO (4 [25]–5 [26] deg).

In order to make sure that these findings are not an *artifact* of our calculations, parallel results were also obtained for N_3^- with basis set 6–31G: in this case, the calculations point without doubt to a linear structure. Our results for N_3^- are also given in Table 2.

3.2 Force Constants and Vibration Frequencies

The second derivatives of the quadratic expansion mentioned in Paragraph 2.4 yield diagonal and non-diagonal stretching and bending force constants; these are

---

[1] The authors are willing to supply further results upon request. These include 123 calculated points with basis set STO-3G and 54 with basis set 6-31G on the molecules HN_3, N_3^-, NH and N_2.

Table 2. Equilibrium geometries[a]

Molecule	Method	Basis set	$R_{N_1N_2}$	$R_{N_2N_3}$	R_{N_3H}	α	β	τ	$R_{N_1N_3}$
HN₃	calc.[b]	STO-3G	1.176	1.285	1.057	103	170	180°	2.452
	calc.[b]	6-31G	1.125	1.272	1.021	111	170	180	2.388
	exp.[e]	—	1.134	1.240	1.021	112.4	180°	180°	2.374
N₃⁻	calc.[b]	6-31G	1.177	1.177	—	—	180	180	2.354
	exp.[f]	—	1.12–1.15[d]	1.12–1.15[d]	—	—	180°	180°	2.24–2.30[d]

[a] Distances in Å, angles in degrees. See Fig. 1 for labelling of N atoms.   [b] This work.   [c] Postulated value.
[d] Solid state results depending on the nature of the crystal.   [e] Ref. [3].   [f] Ref. [23].

Table 3. Determination of β and k_β

Method	Basis set	Analytical fit degree[b]	Coupling	β (deg)	k_β (10^{-12} erg/rad^2)
SCF[a]	STO-3G	2	α, β	170	4.7
SCF[a]	6-31G	2	1st neighb.[c]	170	5.4
SCF[a]	6-31G	3	—	170	5.4
CI[a] ($\delta = 2 \cdot 10^{-4}$)	6-31G	2	—	170	12.6
SCF[a]	6-31G**	2	—	173	6.9
SCF[d]	(4, 4, 3, 2; 4, 3) + pol.	2	—	172	6.8
exp.	—	—	—	180[e]	10.0[f]

[a] This work.   [b] Maximum power of β in polynomial.
[c] See Section 2.1.   [d] Ref. [7].
[e] Ref. [3]. Postulated value.   [f] Ref. [27].

Table 4. Force constants and vibration frequencies

Property	HN$_3$ Calculated[a]	Exp.[d]	N$_3^-$ Calculated[a]	Exp.[e]
k_{11}[b]	21.9	17.3	17.2	13.4
k_{22}	9.3	10.1	17.2	13.4
k_{33}	7.1	6.2	—	—
$k_{\alpha\alpha}$	0.71	0.69	—	—
$k_{\beta\beta}$	0.38	0.71	0.66	0.58
k_τ	0.10	—	—	—
k_{12}	2.4	1.74	2.9	1.74
$k_{1\beta}$	−0.14	0.03	—	—
k_{23}	−0.23	0.30	—	—
$k_{2\beta}$	−0.35	0.06	—	—
$k_{2\alpha}$	1.1	0.44	—	—
$k_{3\alpha}$	0.24	0.04	—	—
$k_{\alpha\beta}$	−0.02	0.12	—	—
$\nu_S(N_1N_2N_3)$[c]	1617	1269.0	1562	1344
$\nu_a(N_1N_2N_3)$	2344	2140.4	2276	2041
$\nu(NH)$	3606	3335.6	—	—
$b(NH)$	982	1152.5	—	—
$b_{in}(N_1N_2N_3)$	472	657.9	693	645
b_{out}	496	740.0	693	645

[a] This work.

[b] Force constant k_{ij} corresponds to internal coordinates R_i and R_j (see (Fig. 1); units are 10^5 dyn/cm.

[c] Approximate description of normal modes is given [27]: ν_s and ν_a corresponds to symmetric and asymmetric stretching respectively, b_{in} and b_{out} to in- and out-of-plane bending. Units are cm^{-1}.

[d] See Ref. [27] for force constants, Refs. [4, 5] for vibration frequencies.

[e] Solid state results depending on the nature of crystal [28].

given in Table 4, and compared with available values derived from measured frequencies. Here again however, due to lack of data, the experimentalists have had to make approximations to derive these constants [27, 28].

Direct comparison of the calculated and measured vibration frequencies, also given in Table 4, shows only fair agreement between the two sets of values: the calculated stretching frequencies are high, whereas the calculated bending frequencies are low. This type of agreement is what one may expect from a non-polarized and a non-correlated wave function. The same applies to the frequencies of N_3^- for which no direct comparison with experiment is possible.

The influence of correlation and of basis set was tested on the β-bending force constant of HN_3, just as it was tested for the value of β. The results are given in the last column of Table 3. We note that inclusion of polarization functions in the basis set as well as that of correlation both tend to increase the force constant. The CI result shows relatively good agreement with the experimental value, which because of the approximations mentioned above should be regarded as tentative only. It is expected that similar CI calculations should reduce the stretching force constants.

3.3. Population Analysis

Mulliken population analyses [29] calculated with the minimal STO-3G basis set are shown in Fig. 2 for HN_3, N_3^-, NH and N_2: net populations are indicated above the atoms, and overlap populations above the bonds.
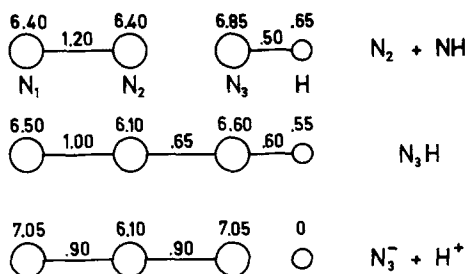

Fig. 2. Mulliken population analysis results. Net populations are indicated above the atoms, overlap populations above the bonds. STO-3G basis set

The data permit a clear visualization of the charge transfers which take place when HN_3 is dissociated, and when N_3^- is protonated.

If one compares the overlap populations of Fig. 2 with those of N_2 (triple bond), N_2H_2 (double bond) and N_2H_4 (single bond) calculated [30] with the same basis set,[2] it is apparent that:

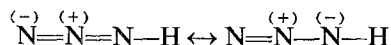1) the N—N bonds in N_3^- correspond closely to double bonds

---

[2]   Respectively 1.20, 0.88 and 0.54 for N_2, N_2H_2 and N_2H_4 [30].

2) the N_1—N_2 and N_2—N_3 bonds in HN_3 correspond to intermediates between a double and a triple bond and a double and a single bond respectively.

Thus N_3^- may be depicted by the formula:

$$\overset{(-)}{N}=N=\overset{(-)}{N}$$
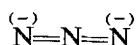
and HN_3 by the resonance structures:

$$\overset{(-)}{N}=\overset{(+)}{N}=N-H \leftrightarrow N=\overset{(+)}{N}-\overset{(-)}{N}-H$$

These structures are in agreement with chemical intuition.

3.4. Dissociation Path

3.4.1. Description

Exploratory calculations of the least-energy dissociation path were carried out with the minimal STO-3G basis set. Simultaneous minimization of the energy as a function of all parameters was made at a few chosen values of R_2. Once the geometries along the reaction path were established with this basis set, calculations with the larger 6-31G (DZ) basis set were carried out to refine the values obtained.

The 6-31G results are given in the first column of Table 1 (first three entries) and are compared to the STO-3G results in Fig. 3. We note that, as for CH_2N_2, basis set STO-3G tends to overestimate systematically the N—N bond distance. This seems to indicate that the STO-3G basis set is not fully optimal for nitrogen.

The potential energy curves shown in the bottom of Fig. 3 represent the energy along the dissociation coordinate (R_2), calculated at the values of the other parameters given in the same figure, except for the 6-31G** results which pertain to the 6-31G geometries. We also note that the minimal STO-3G basis set yields a dissociation energy which is higher than the larger 6-31G basis set; this rather unexpected result may be explained by basis-set-borrowing between NH and N_2.[3] Of more importance is the influence of polarization functions on the dissociation energy. The results of Table 1 and Fig. 3 show that addition of polarization functions (3*d* on N and 2*p* on H) increases the dissociation energy by a factor of two (~ 0.02 a.u. $\rightarrow \sim 0.04$ a.u.). This important effect results from the very large lowering caused by the addition of these functions (-0.11 a.u.) at equilibrium geometry.

3.4.2. Analysis

It is interesting to compare the minimal energy approaches of NH and N_2 on the one hand with those of CH_2 and N_2 on the other hand. In Fig. 4 we give a sketch

---

[3] A study of basis-set-borrowing applied to the dissociation energy of CH_2 into $C + H_2$ has shown that this effect accounts for $\sim 25\%$ of the calculated dissociation energy with basis set STO-3G [31].
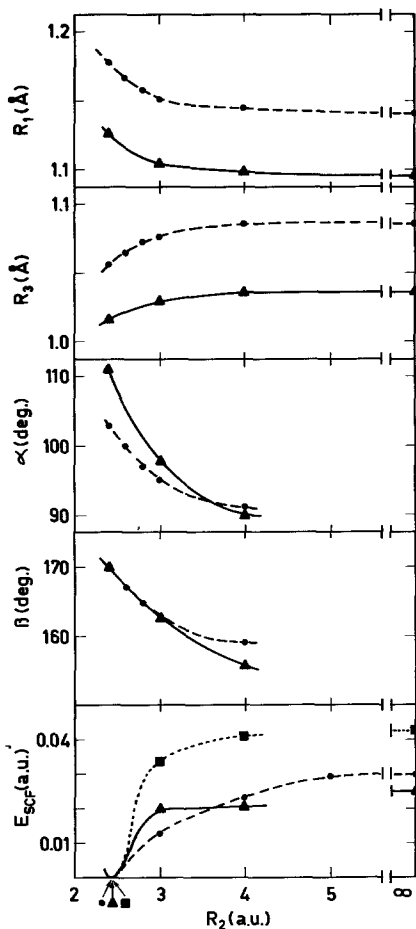
Fig. 3. Geometry optimization along dissociation path. Circles, triangles and squares refer to basis sets STO-3G, 6-31G and 6-31G**, respectively. In the lower part of the figure, the corresponding relative energies are given; the 6-31G** energies refer to 6-31G geometries. Absolute energies at the minimum of the potential surfaces are respectively -161.6659, -163.7292 and -163.8392 a.u. for basis sets STO-3G, 6-31G and 6-31G**

of the two systems together with the angles involved at different distances of approach.

First we notice that at large distances the angles of approach are almost identical: both NH and $CH_2(XH)$ attack the N_2 molecule at an angle of 25° from N—N—X co-linearity. This angle corresponds to a point of attack of lowest electron density which lies between the π-structure and the lone pairs in N_2. The near-perpendicularity between the XH bonds and the N—X direction is also easily understood: in CH_2N_2, the new bond is formed perpendicular to the two CH bonds and the carbon lone pair which all lie in the same plane; in NHN_2 the new bond is formed perpendicular to the NH bond and the two nitrogen lone pairs which are also co-planar.

When the N_2—XH distance decreases, apparently the two systems behave differently: in CH_2N_2, we find that both angles ((H_2)—C—N and N—N—CH_2) increase to 180° at equilibrium resulting in a change from C_s structure to a C_{2v} structure; in
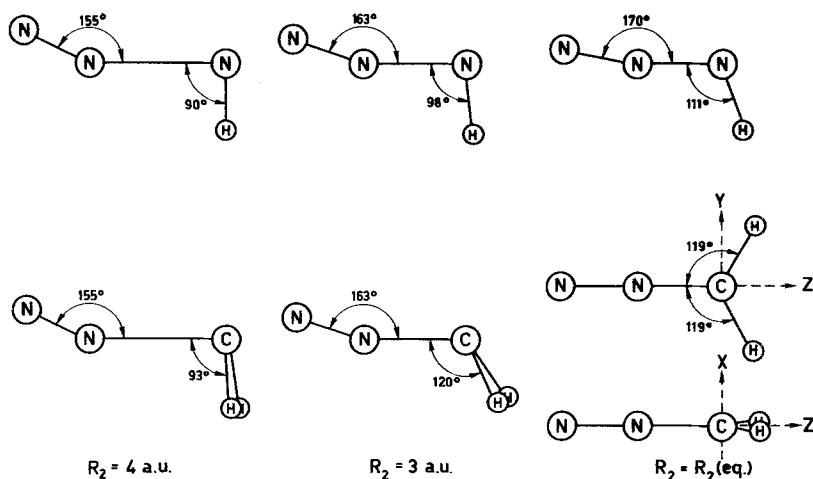
Fig. 4. Comparison of dissociation paths of HN_3 and CH_2N_2 (Ref. [12])

NHN_2, the N—N—H angle increases only to $\sim 110°$, and the N—N—N angle to $\sim 170°$ at equilibrium resulting in no change in symmetry.

The planar C_{2v} structure in CH_2N_2 has been explained [12] on the basis of a strong interaction between the two CH bond densities and a π structure lying above and below the molecular plane. Further the H—C—H angle of $120°$ points to a near sp^2 structure of the carbon electrons; the N—N—C linearity is ensured by a symmetrical interaction between the N—N bond and each of the CH bonds.

In HN_3, there also exists a π structure lying above and below the molecular plane. In this case, however, because NH, contrary to CH_2, has axial symmetry, the π structure can be established in a plane perpendicular to that found for CH_2N_2, i.e. without having to straighten out the N—N—H angle. Thus the near sp^2 bond directions in nitrogen can be maintained on the N_3 atom because a lone-pair lies at $120°$ of the N—H and N_2—N_3 bonds in the molecular plane. This structure also explains the close but nevertheless non-linearity of the N_1—N_2—N_3 angle as being due to an asymmetrical repulsion between the N_1—N_2 bond density with the N_3—H bond density on the one hand and the N_3 lone-pair on the other hand.

3.5. CI *Calculations*

CI calculations (6-31G basis set) were made at a few points along the dissociation path ($R_2 = 2.4$, 3.0, 4.0 and 6.0 a.u.) at chosen values of the interaction threshold (cf. Sect. 2.3). In Table 1, some of the calculated energies are given.

The CI results change the adiabatic dissociation energy of the $^1A'$ state by 10 kcal/mole, but do not modify the nature of the dissociation products,

i.e. $NH(\frac{1}{2}\,^1\Delta + \frac{1}{2}\,^1\Sigma^+)$. The reason for this is that the ground $^1A'$ state (Conf. *A*) was chosen as reference state for these calculations over the whole range of R_2 at the expense of Configuration *C*; thus the 50% mixture of Configurations *A* and *C* necessary to the description of $NH(^1\Delta)$ was not achieved. For example, at $R_2 = 6.0$ a.u. the weights (square of CI coefficients) of Configurations *A* and *C* in the CI expansion are respectively 0.907 and 0.005.

In order to obtain a correct dissociation limit, calculations were carried out on NH alone at the same level of approximation. One CI calculation was based on the orbital energies and transformed molecular integrals generated by a Fock matrix corresponding to a $^3\Sigma^-(1\sigma^2 2\sigma^2 3\sigma^2 1\pi_x 1\pi_y)$ structure, which ensures a $\pi_x - \pi_y$ degeneracy. Also, the reference state for the selection of the interacting configurations was chosen as: $(1/\sqrt{2})(|\cdots \bar{\pi}_x \pi_x| - |\cdots \bar{\pi}_y \pi_y|)$ in accordance with the $^1\Delta$ irreducible representation.[4] Another calculation on NH similar to that on HN_3 was made, i.e. both the SCF and CI reference state was chosen as $\frac{1}{2}(^1\Sigma^+ + \,^1\Delta)$ $(1\sigma^2 2\sigma^2 3\sigma^2 1\pi_x^2)$. The results of these two calculations are given in Table 1.

Since the $\pi_x - \pi_y$ degeneracy is due to the axial symmetry of NH alone the effect of this degeneracy is apparent only at the dissociation limit ($R_2 > 6.0$ a.u.) and disappears at the equilibrium geometry of HN_3 ($R_2 = 2.4$ a.u.). Thus the difference between the energies of the two CI calculations gives a quantitative correction to the dissociation energy of HN_3.

3.6. Estimation of the Dissociation Energy of N_3H

From the data given in previous sections it is possible to estimate roughly the dissociation energy of HN_3.

First we consider the process:

$$HN_3(^1A') \rightarrow N_2(^1\Sigma_g^+) + NH(\tfrac{1}{2}\,^1\Delta + \tfrac{1}{2}\,^1\Sigma^+).$$
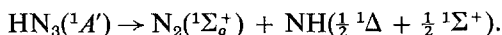
The CI results (6-31G) yield 25 kcal/mole for this reaction. Addition of polarization function to the basis set adds 11 kcal to this value at the SCF level of approximation (cf. Fig. 3) and, by analogy to similar calculations [26], it is estimated to add a further 4 kcal/mole for their contribution to the CI expansion. Thus 40 kcal/mole seems a reasonable estimate for the energy of the above process.

This energy should be reduced by 6 kcal/mole in order to take into account the difference in energy between $NH(\frac{1}{2}\,^1\Delta + \frac{1}{2}\,^1\Sigma^+)$ and $NH(^1\Delta)$ as discussed in Sect. 3.5. Thus the reaction:

$$HN_3(^1A') \rightarrow N_2(^1\Sigma_g^+) + NH(^1\Delta)$$
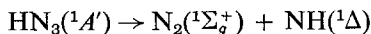
is endothermic by ~ 35 kcal/mole.

---

[4]   In fact $\Psi(^1\Delta^\pm) = \frac{1}{2}(|\cdots \bar{\pi}_x \pi_x| - |\cdots \bar{\pi}_y \pi_y| \pm i(|\cdots \pi_x \bar{\pi}_y| - |\cdots \bar{\pi}_x \pi_y|))$ however it may be shown that, because of the inherent equality $J(\pi_x \pi_x) - J(\pi_x \pi_y) = 2K(\pi_x \pi_y)$, either the real or the imaginary part of the wavefunction is sufficient to describe adequately the $^1\Delta$ state. This point was tested numerically here.

The thermodynamic dissociation energy may be estimated from the above value by considering the term energy of $NH(^1\Delta)$ together with zero-point energies. Using the experimental value $T_e(^1\Delta) = 1.57$ eV [34] together with the vibration frequencies calculated here for HN_3 and the corresponding experimental values for N_2 [35] and $NH(^3\Sigma^-)$ [36] yields:

$$HN_3(^1A') \rightarrow N_2(^1\Sigma_g^+) + NH(^3\Sigma^-)\Delta H_0^0 \sim -8 \text{ kcal/mole.}$$
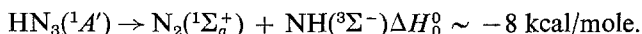
Therefore, according to the present estimate, hydrazoic acid should be slightly metastable. This conclusion is contrary to electron-impact measurements [6] which predict a value of $+9$ kcal/mole for the same process. At the present time, because of the approximate nature of our calculated value, as well as of experimental uncertainties due to the exact nature of the fragments, it is difficult to predict with certainty whether HN_3 is stable or metastable.

However, our findings seem to account better for the explosive nature of the molecule. According to preliminary calculations on the $^3A''$ state, which correlates with $N_2(^1\Sigma_g^+) + NH(^3\Sigma^-)$, the intersystem crossing with the ground $^1A'$ state occurs at energies close to the $^1A'$ state dissociation limit. As a result, there should be a ~ 30 kcal/mole potential barrier towards dissociation of the molecule. These numbers provide an explanation to the chemical properties of the molecule: it is capable of explosive decomposition at moderate temperatures, but nevertheless can be stored as a gas at room temperature and low pressure.

4. Conclusions

The present study on hydrazoic acid gives information on the structure of this molecule, and offers some insight as to its dissociation mechanism. Obviously more work will be necessary to obtain reliable quantitative results on the energetics of its dissociation. This work will be pursued in the following two directions:

a) More elaborate SCF CI calculations including polarization functions in the basis set will be made in order to confirm (or infirm) the present estimates.

b) With these improved wavefunctions, we plan to calculate the spin-orbit interaction allowing the molecule to pass from the $^1A'$ state to the $^3A''$ state.

References

1. Roberts, J. D., Caserio, M. C.: Basic principles of organic chemistry. New York: Benjamin 1965
2. Shapiro, E. L.: Chem. Eng. News **52**, 5 (1974)
3. Amble, E., Dailey, B. P.: J. Chem. Phys. **8**, 135 (1939)
4. Davies, M. M.: Trans. Faraday Soc. **35**, 1184 (1939)
5. Eyster, E. H., Gillette, R. H.: J. Chem. Phys. **8**, 369 (1940)
6. Franklin, J. L., Dibeler, V. H., Reese, R. M., Krauss, M.: J. Am. Chem. Soc. **80**, 298 (1957)
7. Harrison, S. W., Fischer, C. R., Kemmey, P. J.: Chem. Phys. Letters **36**, 229 (1975)

8. Wyatt, J. F., Hillier, I. H., Saunders, V. R., Connor, J. A.: J. Chem. Phys. **54**, 5311 (1971)
9. Lee, T. H., Colton, R. J., White, M. G., Rabalais, J. W.: J. Am. Chem. Soc. **97**, 4845 (1975)
10. Bonaccorsi, R., Petrongolo, C., Scrocco, E., Tomasi, J.: J. Chem. Phys. **48**, 1500 (1968)
11. Lievin, J., Verhaegen, G.: Theoret. Chim. Acta (Berl.) **42**, 47 (1976)
12. Lievin, J., Verhaegen, G.: Theoret. Chim. Acta (Berl.) **45**, 269 (1977)
13. Hehre, W. J., Latham, W. A., Ditchfield, R., Newton, M. D., Pople, J. A.: GAUSSIAN 70, Program No. 236, Q.C.P.E.
14. Roothaan, C. C. J.: Rev. Mod. Phys. **23**, 69 (1951)
15. Davidson, E. R.: Chem. Phys. Letters **21**, 565 (1973)
16. Morokuma, K., Iwata, S.: private communication
17. Hehre, W. J., Stewart, R. F., Pople, J. A.: J. Chem. Phys. **51**, 2657 (1969)
18. Hehre, W. J., Ditchfield, R., Pople, J. A.: J. Chem. Phys. **56**, 2257 (1972)
19. Hariharan, P. C., Pople, J. A.: Theoret. Chim. Acta (Berl.) **28**, 213 (1973)
20. Binkley, J. S., Whitehead, R. A., Hariharan, P. C., Seeger, R., Pople, J. A.: GAUSSIAN 76, Program No. 368, Q.C.P.E.
21. Whitten, J. L., Hackmeyer, M.: J. Chem. Phys. **51**, 5584 (1969)
22. Decius, J. C.: J. Chem. Phys. **16**, 1025 (1948)
23. Frevel, L. K.: J. Am. Chem. Soc. **58**, 779 (1936)
24. Cox, A. P., Thomas, L. F., Sheridan, J.: Nature (London) **181**, 1000 (1958)
25. Poppinger, D., Radom, L., Pople, J. A.: J. Am. Chem. Soc. **99**, 7806 (1977)
26. McLean, A. D., Loew, G. H., Berkowitz, D. S.: J. Mol. Spectry. **64**, 184 (1977)
27. Orville Thomas, W. J.: Trans. Faraday Soc. **49**, 855 (1953)
28. Gray, P., Waddington, T. C.: Trans. Faraday Soc. **53**, 901 (1957)
29. Mulliken, R. S.: J. Chem. Phys. **23**, 1833 (1955)
30. Sana, M.: Ph.D. Thesis, Université Catholique de Louvain (1975)
31. Neisius, D., Verhaegen, G.: unpublished results
32. Salem, L., Leforestier, C., Segal, G., Wetmore, R.: J. Am. Chem. Soc. **97**, 479 (1975)
33. Gervy, D., Verhaegen, G.: Intern. J. Quantum Chem. **12**, 115 (1977)
34. Lents, J. M.: J. Quantum Spectry. Radiat. Transfer **13**, 297 (1973)
35. Herzberg, G.: Spectra of diatomic molecules. Princeton, New Jersey: Van Nostrand 1950
36. Guenebaut, H.: J. Phys. **16**, 1405 (1965)